Crossed Andreev Reflection in Zigzag Phosphorene Nanoribbon Based Ferromagnet/Superconductor/Ferromagnet Junctions

Ruigang Li
Guangzhou University
Lei Chen
Beijing University of Civil Engineering and Architecture
Jun-Feng Liu (phjfliu@gzhu.edu.cn)
Guangzhou University
Jun Wang
Southeast University

Research Article

Keywords: crossed Andreev reflection, electron tunneling, superconductor

Posted Date: January 3rd, 2022

DOI: https://doi.org/10.21203/rs.3.rs-1209980/v1

Version of Record: A version of this preprint was published at Scientific Reports on April 12th, 2022. See the published version at https://doi.org/10.1038/s41598-022-10086-2.

Crossed Andreev Reflection in Zigzag Phosphorene Nanoribbon Based Ferromagnet/Superconductor/Ferromagnet Junctions

Ruigang Li[1], Lei Chen[2], Jun-Feng Liu[1,*], and Jun Wang[3,†]

[1]Department of Physics, School of Physics and Materials Science, Guangzhou University, Guangzhou 510006, China
[2]College of Science, Beijing University of Civil Engineering and Architecture, Beijing 100044, China
[3]Department of Physics, Southeast University, Nanjing 210096, China
[*]phjfliu@gzhu.edu.cn
[†]jwang@seu.edu.cn

ABSTRACT

We study the crossed Andreev reflection in zigzag phosphorene nanoribbon based ferromagnet/superconductor/ferromagnet junction. Only edge states, which are entirely detached from the bulk gap, involved in the transport process. The perfect crossed Andreev reflection, with the maximal nonlocal conductance $-2e^2/h$, is addressed by setting the chemical potentials of the leads properly. At this situation, the local Andreev reflection and the electron tunneling are completely eliminated, the incoming electrons can only be reflected as electrons or transmitted as holes, corresponding to the electron reflection and the crossed Andreev reflection respectively.The nonlocal conductance oscillates periodically with the length and the chemical potential of the superconductor. Our study shows that the phosphorene based junction can be used as the quantum device to generate entangled-electrons.

Introduction

In a superconductor junction, the nonlocal coupling between two electrons from different leads forms the crossed Andreev reflection (CAR)[1]. It is desirable to find electronic devices with a large probability and convenient manipulation of CAR, as the reversed process of CAR is practical in generating nonlocal entangled-electrons[2–4]. Nowadays, the normal/superconductor/normal (N/S/N) junction had been used to detect CAR[5,6], where the superconductor in the junction can be induced by the proximity effect.At the same time, the discovery of graphene[7–10] become a breakthrough in the field of two-dimensional material. Studies of CAR in graphene based superconductor junctions were reported since then. J. Cayssol[11] proposed a graphene based N/S/N junction and point out that the transmission of CAR acts as a function of the length of the narrow superconductor region. X. Wu et al.[12] found that a cooper pair split into two nonlocal electrons perfectly in a superconductor junction based on a bilayer graphene spin valve. Besides spin, they stressed that such two electrons are also involved in valley entanglement. R. Beiranvand et al.[13] provided a new way to create equal spin electron entanglement by studying the anomalous CAR in a graphene based junction, where the device is consist of a triplet pairing superconductor. In reference[14], researchers examine the CAR in EuO-graphene superconductor junction, where the graphene lead and device region would be induced to a ferromagnet and superconductor by the proximity effect respectively. They found that the pure CAR oscillates rapidly and periodically with the length of the device. Besides bulk graphene, a CAR study of graphene nanoribbon junctions has also been reported. L. Zhang et. al[15] proposed a ferromagnetic/superconductor junction based on zigzag graphene nanoribbon, and point out that the CAR in such junction is controllable by changing the direction of the ensemble magnet.

Recently, phosphorene[16–18], a graphene-like two-dimensional material, had been successfully isolated. Like graphene, the honeycomb structure of phosphorene nanoribbon provides two distinct nanoribbons: armchair and zigzag nanoribbon. The armchair nanoribbon is a gapped semiconductor, while the zigzag one contains four degenerate quasi-flat edge bands detached from the bulk bands, considering spin degeneracy[20]. As we know, the electronic properties of zigzag phosphorene nanoribbon (ZPR) are dominated by the edge bands at low energy region. Because the electrons in the edge bands are localized to the edges, it can be easily controlled by an external field, especially by the electric field[21]. Furthermore, the edge bands are entirely detached from the bulk bands, which helps them to eliminate the trouble caused by the bulk bands. Such magnificent properties of edge bands make it good for building the electronic device. Noted that the Josephson effect in phosphorene based

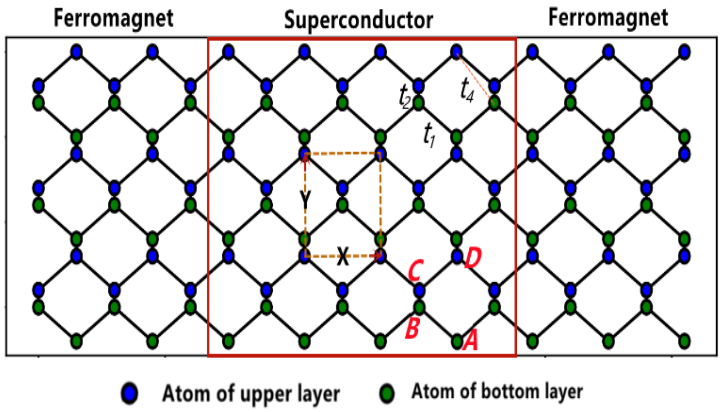

Figure 1. Schematic of the ferromagnet/superconductor/ferromagnet junction based on zigzag phosphorene nanoribbon.

superconductor junctions were investigated[19]. Researchers explain the strong anisotropic supercurrent of Josephson effect comes from the number differences of Andreev bound states. Besides the direction, the supercurrent is also affected by the chemical potential and the length of the superconductor region.

However, compared to graphene, according to our investigation, the study of CAR in phosphorene based junction is still a few.In this Letter,we study the crossed Andreev reflection in zigzag phosphorene nanoribbon based ferromagnet/superconductor/-ferromagnet (F/S/F) junction. The ferromagnetism and the superconductor in phosphorene nanoribbon can be achieved in proximity to EuO[22] and s-wave superconductor respectively. According to the first principle calculation, the exchange energy can reach 184 meV. Normally, the electron tunneling (ET) and local Andreev reflection (LAR) will compete with the CAR in the scattering process inevitably[23], making the nonlocal transmission weaken. In our study, the scattering process in the junction can be consisted of CAR and electron reflection (ER), where the ET and LAR are completely blocked by setting the chemical potentials of both leads properly. The maximal nonlocal conductance of CAR can reach $-2e^2/h$, corresponding to a perfect CAR. Also, we found out that the nonlocal conductance is oscillating periodically with the length and chemical potential of the superconductor. Our finding shows that the phosphorene based junction can be used as the quantum device to generate entangled-electrons.

This work is organized as follows. The structure and model of the junction are presented in section 2; the calculation results and the corresponding analysis are presented in section 3. In section 4, the conclusion of this work is given.

Structure and model

Fig.1 is the structure we studied. The F/S/F junction is based on ZPR, with the superconductor connected to two ferromagnetic leads. The ferromagnet and superconductor can be achieved by the proximity effect. The primitive cell is shown in the regular frame with the size $X \times Y$, where $X = 3.27$ Å and $Y = 4.43$ Å are the length of the cell in x and y direction respectively. The size of the device region is $L \times T = N_L X \times N_T Y$, where N_L and N_T denote the number of unit cell in x and y direction respectively. For a convenient description, N_L is referred to as the length of the device region. As we know, the effective Hamiltonian of the bare phosphorene nanoribbon can be written in a tight binding form

$$H_0 = \sum_{ABCD} t_1(c^\dagger_{A\sigma}c_{B\sigma} + c^\dagger_{C\sigma}c_{D\sigma}) + t_2(c^\dagger_{A\sigma}c_{D\sigma} + c^\dagger_{B\sigma}c_{C\sigma}) + \sum_{\langle i,j\rangle} t_4(c^\dagger_{i\sigma}c_{j\sigma}) + H.c.$$

where $c_{i\sigma}$ ($c_{A\sigma}$, $c_{B\sigma}$, $c_{C\sigma}$, $c_{D\sigma}$) denotes annihilating an electron on site i (A,B,C,D) of the unit cell, σ is the spin of the electron. There are 3 hopping parameters in H_0, which also shown in Fig.1. The parameters are set to be $t_1 = -1.220$ eV, $t_2 = 3.665$ eV, $t_4 = -0.105$ eV. Noted that, compare with the model in reference[24], t_3 and t_5 are neglected, because they are much smaller than t_1 and bring no important effect on the transport properties of phosphorene nanoribbon. $\langle i,j\rangle$ in H_0 denotes that an electron or a hole hops from atom j in one layer to atom i in another layer, with a longer distance than t_2 hopping, which is shown in Fig.1.

Bogliubov-de Gennas (BdG) equation is used to study the CAR in ZPR superconductor junction in this work. The

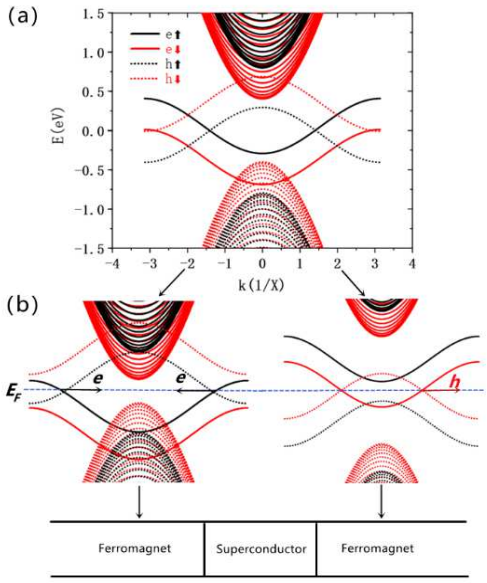

Figure 2. (a) The band structure of the ferromagnetic lead with $\mu = 0$. (b) Band structures of left and right ferromagnetic lead with $\mu_1 > 0$ and $\mu_2 < 0$ respectively.

tight-binding Hamiltonian of the junction can be written as

$$H = H_S + H_F + H_T$$

$$H_{\uparrow/\downarrow} = H_{0\uparrow/\downarrow} \pm H_{\mathrm{ex}}$$

$$H_T = \sum_{<F,S>} \mathrm{t_1 c_S}^{+} \mathrm{c_F} + H.c$$

$$H_S = \begin{pmatrix} H_{0\uparrow} - \mu_s & 0 & 0 & \Delta \\ 0 & H_{0\downarrow} - \mu_s & -\Delta & 0 \\ 0 & -\Delta^* & \mu_s - H_{0\uparrow} & 0 \\ \Delta^* & 0 & 0 & \mu_s - H_{0\downarrow} \end{pmatrix}$$

$$H_F = \begin{pmatrix} H_{\uparrow} - \mu & 0 & 0 & 0 \\ 0 & H_{\downarrow} - \mu & 0 & 0 \\ 0 & 0 & \mu - H_{\uparrow} & 0 \\ 0 & 0 & 0 & \mu - H_{\downarrow} \end{pmatrix}$$

H_T stands for the couple between superconductor region and ferromagnetic leads, where $c_S^{\dagger} c_F$ represents a particle hops from the lead to the device region, and $\langle F, S \rangle$ denotes the hopping happens between nearest atoms. H_S/H_F denotes the Hamiltonian of superconductor/Ferromagnet. Δ in H_S is the order parameter of the superconductor. $H_{0\uparrow(\downarrow)}$ in H_S/H_F denotes the Hamiltonian of spin-up (down) electrons without exchange field. H_{ex} in H_F represents the exchange energy in the ferromagnetic leads, and the value of H_{ex} is set to be 0.2 eV in this study. μ/μ_s is the chemical potential of the ferromagnetic lead/superconductor region, which can be tuned by a top gate voltage.

The calculation in this study is done by Kwant[25], a software for quantum transport calculation. The tight-binding model of the system can be built by Kwant's package, and the structure can be visualized by setting system parameters. After that, the scattering matrix $[S]$ can be obtained. In our study, the expression of the wave function in the right lead is $\sum_e S_{eh}(E_F)\,\psi_e$, where e denotes the injecting electron modes in the left lead, h denotes the outgoing hole mode in the right lead and E_F is the Fermi energy. The element of scattering matrix S_{eh} denotes the CAR process, and the transmission between the electron in the left lead and the hole in the right lead can be written as $T_{eh} = |S_{eh}(E_F)|^2$. According to the reference[26], the nonlocal conductance of CAR can be given as

$$\mathrm{G} = \left[\frac{dI_R}{dV_L}\right]_{V_R=0} = -\frac{\mathrm{e}^2}{\mathrm{h}}\,\mathrm{T}_{eh}$$

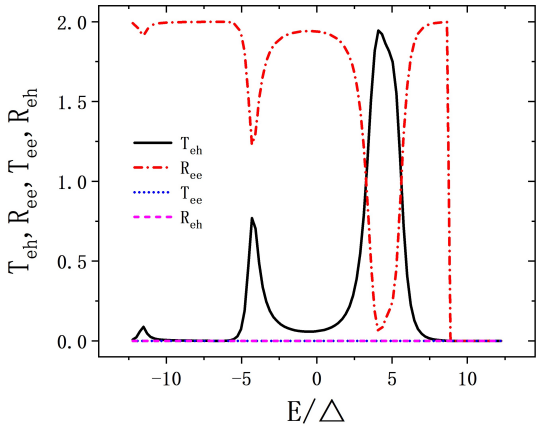

Figure 3. The scattering coefficients of CAR, ER, ET and LAR, the parameters of the junction are setting as: $N_T = 40$, $N_L = 40$, $\mu_s = 0.164$ meV, $\mu_1 = 0.4$ eV, $\mu_2 = -0.6$ eV.

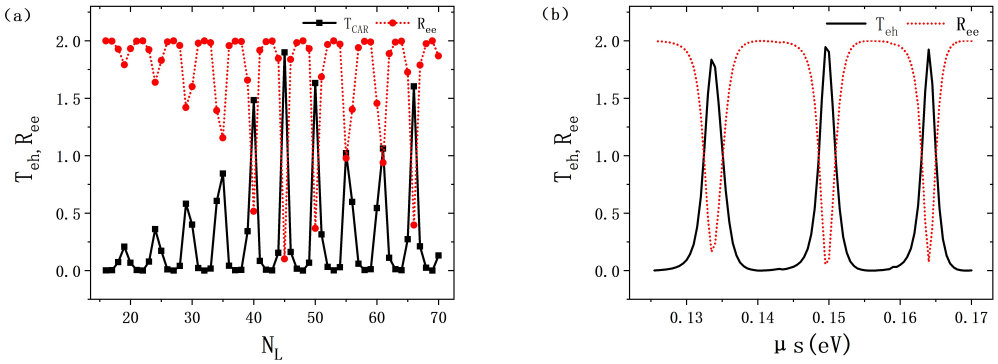

Figure 4. The scattering coefficients of CAR and ER as a function of (a) the length (N_L) and (b) the chemical potential (μ_s) of the superconductor.

where I_R and V_L can be measured as the current and the applied bias voltage in the left or right lead respectively. Kwant solve the linear equations and obtained the wavefunctions directly from the tight-binding model, this feature makes the calculation speed faster than the lattice Green function approach. For more details please refer to reference[25].

Results and discussion

The band structures of the ferromagnetic lead had been shown in Fig.2. The electronic and hole bands are drawn together, which are plot in solid and dot lines respectively. Noted that, there exist four electron (hole) edge bands in the band gap, considering the spin degeneracy. The electron edge bands are separated into two double degenerate bands by the exchange field, which can be found in Fig.2(a). Without losing generality, the upper/bottom edge bands are set to be the spin-up/down bands. Here, we set $\mu_1 > 0$ and $\mu_2 < 0$ to get the band structure of left and right lead in Fig.2(b). According to the Hamiltonian of the ferromagnetic lead, when the chemical potential is set to be $\mu > 0$, the electron bands will be pushed down and the hole bands will be uplifted. By doing so, the LAR and ET can be eliminated in the scattering process. This can be understood from Fig.2(b), at the Fermi energy E_F, there are no conducting modes to reflect holes and transmit electrons. Suppose there is no spin flipping in the process, the bands of spin-up hole and the spin-down electron will not conducting, even though there exist modes for these two bands at the Fermi energy. Therefore, only two situations happen when electrons injecting into the system: reflect electrons or transmit holes for forming ER or CAR respectively.

The calculation results are shown in Fig.3. The number of unit cell of the device region are $N_L = 40$, $N_T = 40$. The chemical potential of left (right) lead is set to be $\mu_1 = 0.4$ eV ($\mu_2 = -0.6$ eV), so that there is only spin-up electron injecting into the

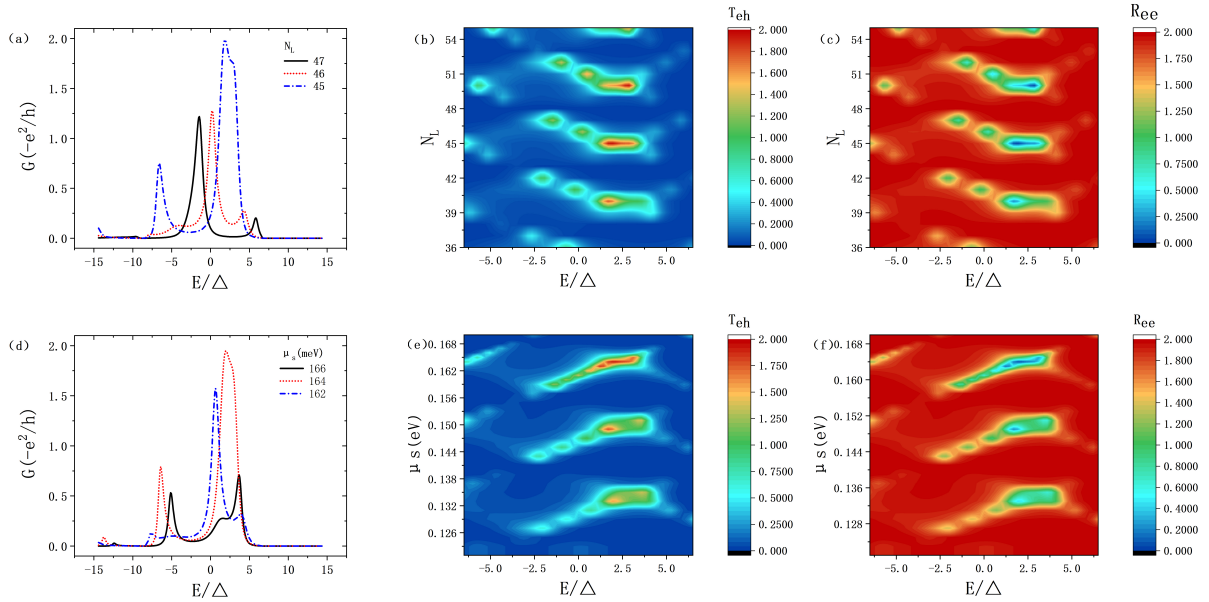

Figure 5. (a) The nonlocal conductance for $N_L = 45$, 46 and 47. (b)/(c) The transmission/reflection of CAR/ER as a function of N_L and the Fermi energy E, with the μ_s kept constant. (d) The nonlocal conductance for $\mu_s = 162$, 164 and 166 meV. (e)/(f) The transmission/reflection of CAR/ER as a function of μ_s and the Fermi energy E, with the N_L kept constant.

system around $E = 0$ eV. The chemical potential and the superconductor gap of the superconductor are set to be $\mu_s = 164$ meV and $\Delta = 1.5$ meV respectively. Agree with our analysis above, the scattering coefficients of LAR and ET are zero, i.e., $R_{eh} = 0$ and $T_{ee} = 0$, for there is no modes for these two process around $E = 0$ eV. Since there are two electrons injecting into the junction simultaneously and only CAR and ER existed in the scattering process at the energy range we studied, $T_{eh} + R_{ee} = 2$. We found that the scattering coefficient in Fig.3 is asymmetric along with the x coordinates, this is due to the asymmetric choice of μ of different lead. Two peaks of T_{eh} appear at $E = -4\Delta$ and $E = 4\Delta$ in Fig.3, with the values 0.75 and 2 respectively. Noted that, the maximal T_{eh} can achieve 2 at $E = 4\Delta$, corresponding to the nonlocal conductance $-2e^2/h$. Such phenomenon is referred to as the perfect CAR, where the incoming electrons from one lead are entirely converting to outgoing holes in another lead.

Fig.4 show the CAR and ER as a function of the length N_L and the chemical potential μ_s of superconductor. By the way, because the band gap of ZPR is barely changed with the transverse size of the junction, the change of the transverse size of the junction cause no much effect on CAR, the results are not shown here. Therefore, the width of the junction is fixed at $N_T = 40$ in this study. The calculation results are shown in Fig.4. In Fig.4(a), T_{eh} as a function of N_L, with μ_s and E are fixed at 149 meV and 2.16Δ respectively. As we see in Fig.4(a), the T_{eh} and R_{ee} are oscillating periodically with N_L, with the period $\Delta N_L = 5$. The value of peaks of both T_{eh} and R_{ee} are changing with N_L. We also found that there exists a peak at N_L= 45, with $T_{eh} = 2$, in Fig.4(a).

Then, when we change μ_s and fix $N_L = 40$ and $E = 2.16\Delta$, a similar effect happens. The T_{eh} oscillates with a period $\Delta\mu_s = 15$ meV, which means that the CAR is quite sensitive to the change of chemical potential of the superconductor. We also found $T_{eh} = 2$ around $\mu_s = 164$ meV. The perfect CAR in Fig.4 is attributed to the resonance effect of the quantum transport, which is related to the relation between the wave vector and the length of the device region. These properties make the CAR in the junction controllable.

The nonlocal conductance of CAR are presented at Fig.5(a) and (d). In Fig.5(a), when N_L increases from 45 to 47, the CAR peak moves from the higher energy to a lower one, with the value changing. Such phenomenon also happens in changing μ_s, which is shown in Fig.5(d). These properties can be easily found in Fig.5(b) and (e). When the energy is in the range $[-7.5\Delta, 7.5\Delta]$, there is a canductance "gap" at $N_L = 43/48/53$ and μ_s around 138/153/168 meV, the corresponding T_{eh} are suppressed and close to zero. Considering Fig.5(b)/(e) and (c)/(f), the T_{eh} and R_{ee} are complementary, with $T_{eh} + R_{ee} = 2$.

Conclusion

In this work, we studied the crossed Andreev reflection in the ferromagnet/superconductor/ferromagnet junction based on zigzag phosphorene nanoribbon. By setting the chemical potential of both leads differently, the scattering process consists of

electron reflection and crossed Andreev reflection, where the local Andreev reflection and electron tunneling are suppressed. The maximal nonlocal conductance of CAR can reach $-2e^2/h$, which is referred to as the perfect CAR. We also found that the transmission coefficient of crossed Andreev reflection oscillates periodically with the length and the chemical potential of the superconductor. These properties make the CAR controllable. Our finding will be helpful to devise the quantum device for generating entangled-electrons.

Acknowledgements

The work described in this paper is supported by National Natural Science Foundation of China (NSFC, Grant Nos. 12174077, Grant Nos. 12174051), and National Natural Science Foundation of Guangdong Province (Grant No. 2021A1515012363). Lei Chen thanks the support by the general Program of Science and Technology Development Project of Beijing Municipal Education Commission No. KM201910016002.

Author contributions statement

R. L., J.-F. L., and J. W. conceived the study. R. L. performed the numerical calculations and wrote the main manuscript text. J.-F. L. improved the manuscript. All authors contributed to discussion and reviewed the manuscript.

References

1. Byers, J. M. & Flatté, M. E. Probing spatial correlations with nanoscale two-contact tunneling. *Phys. Rev. Lett.* **74**, 306–309, DOI: 10.1103/PhysRevLett.74.306 (1995).
2. Samuelsson, P., Sukhorukov, E. V. & Büttiker, M. Quasi-particle entanglement: Redefinition of the vacuum and reduced density matrix approach. *New J. Phys.* **7**, DOI: 10.1088/1367-2630/7/1/176 (2005).
3. Prada, E. & Sols, F. Entangled electron current through finite size normal-superconductor tunneling structures. *Eur. Phys. J. B* **40**, DOI: 10.1140/epjb/e2004-00284-8 (2004).
4. Lesovik, G. B., Martin, T. & Blatter, G. Electronic entanglement in the vicinity of a superconductor. *Eur. Phys. J. B* **24**, DOI: 10.1007/s10051-001-8675-4 (2001).
5. Islam, S. K., Dutta, P. & Saha, A. Enhancement of crossed Andreev reflection in a normal-superconductor-normal junction made of thin topological insulator. *Phys. Rev. B* **96**, DOI: 10.1103/PhysRevB.96.155429 (2017).
6. Celis Gil, J. A., Gomez, P. S. & Herrera, W. J. Noise cross-correlation and Cooper pair splitting efficiency in multi-teminal superconductor junctions. *Solid State Commun.* **258**, DOI: 10.1016/j.ssc.2017.04.009 (2017).
7. Castro Neto, A. H., Guinea, F., Peres, N. M., Novoselov, K. S. & Geim, A. K. The electronic properties of graphene. *Rev. Mod. Phys.* **81**, 109–162, DOI: 10.1103/RevModPhys.81.109 (2009). 0709.1163.
8. Geim, A. K. & Novoselov, K. S. The rise of graphene. *Nat. Mater.* DOI: 10.1038/nmat1849 (2007). 0702595v1.
9. Ferrari, A. C. *et al.* Raman spectrum of graphene and graphene layers. *Phys. Rev. Lett.* **97**, DOI: 10.1103/PhysRevLett.97.187401 (2006).
10. Lee, C., Wei, X., Kysar, J. W. & Hone, J. Measurement of the elastic properties and intrinsic strength of monolayer graphene. *Science* **321**, DOI: 10.1126/science.1157996 (2008).
11. Cayssol, J. Crossed Andreev reflection in a graphene bipolar transistor. *Phys. Rev. Lett.* **100**, DOI: 10.1103/PhysRevLett.100.147001 (2008). 0801.2292.
12. Wu, X. *et al.* Tunable nonlocal valley-entangled Cooper pair splitter realized in bilayer-graphene van der Waals spin valves. *Phys. Rev. B* **101**, DOI: 10.1103/PhysRevB.101.125406 (2020).
13. Beiranvand, R., Hamzehpour, H. & Alidoust, M. Nonlocal Andreev entanglements and triplet correlations in graphene with spin-orbit coupling. *Phys. Rev. B* **96**, DOI: 10.1103/PhysRevB.96.161403 (2017). 1710.00840.
14. Ang, Y. S., Ang, L. K., Zhang, C. & Ma, Z. Nonlocal transistor based on pure crossed Andreev reflection in a EuO-graphene/superconductor hybrid structure. *Phys. Rev. B* **93**, DOI: 10.1103/PhysRevB.93.041422 (2016). 1601.03111.
15. Zhang, L., Tian, H. Y. & Wang, J. Nonlocal conductance control of a zigzag F/S/F graphene nanoribbon junction. *EPL* **98**, DOI: 10.1209/0295-5075/98/47012 (2012).
16. Li, L. *et al.* Black phosphorus field-effect transistors. *Nat. Nanotechnol.* **9**, DOI: 10.1038/nnano.2014.35 (2014).
17. Jia, Y., Xia, F. & Wang, H. layered material for optoelectronics and electronics. *Nat. Commun.* **5**, 1–6, DOI: 10.1038/ncomms5458 (2014).

18. Castellanos-Gomez, A. *et al.* Isolation and characterization of few-layer black phosphorus. *2D Mater.* **1**, DOI: 10.1088/2053-1583/1/2/025001 (2014).

19. Linder, J. & Yokoyama, T. Anisotropic Andreev reflection and Josephson effect in ballistic phosphorene. *Phys. Rev. B* **95**, DOI: 10.1103/PhysRevB.95.144515 (2017). 1702.06125.

20. Peng, X. *et al.* Phosphorene nanoribbons. DOI: 10.1209/0295-5075/108/47005 (2014).

21. Zhou, B., Zhou, B., Zhou, X. & Zhou, G. Even-odd effect on the edge states for zigzag phosphorene nanoribbons under a perpendicular electric field. *J. Phys. D: Appl. Phys.* **50**, DOI: 10.1088/1361-6463/aa52b5 (2017).

22. Chen, H., Li, B. & Yang, J. Proximity Effect Induced Spin Injection in Phosphorene on Magnetic Insulator. *ACS Appl. Mater. Interfaces* **9**, DOI: 10.1021/acsami.7b11454 (2017).

23. Falci, G., Feinberg, D. & Hekking, F. W. Correlated tunneling into a superconductor in a multiprobe hybrid structure. *Europhys. Lett.* **54**, 255–261, DOI: 10.1209/epl/i2001-00303-0 (2001). 0011339.

24. Ezawa, M. Topological origin of quasi-flat edge band in phosphorene. *New J. Phys.* **16**, DOI: 10.1088/1367-2630/16/11/115004 (2014).

25. Groth, C. W., Wimmer, M., Akhmerov, A. R. & Waintal, X. Kwant : a software package for quantum transport scattering region lead 0 lead 2 lead 1. 1–19 (2014).

26. Zhang, S. B. & Trauzettel, B. Perfect Crossed Andreev Reflection in Dirac Hybrid Junctions in the Quantum Hall Regime. *Phys. Rev. Lett.* **122**, DOI: 10.1103/PhysRevLett.122.257701 (2019).